Properties of vortex lattices are of broad interest in superfluids, superconductors, and even astrophysics. Fluctuations in the rotation rate of pulsars are attributed to the dynamics of the vortex lattice in a superfluid neutron liquid (*5*, *31*). Our experiments show that vortex formation and self-assembly into a regular lattice is a robust feature of rotating BECs. Gaseous condensates may serve as a model system to study the dynamics of vortex matter, in analogy to work in type-II superconductors (*32*). Of particular interest are collective modes of the lattice. In liquid helium, transverse oscillations in a vortex lattice (Tkachenko oscillations) have already been investigated (*33*, *34*). Further studies may address the nucleation, ordering, and decay of lattices, in particular to delineate the role of the thermal component (*5*), and possible phase transition associated with melting and crystallization.

References and Notes

1. H. Träuble, U. Essmann, *Phys. Lett.* **24A**, 526 (1967).
2. E. J. Yarmchuk, M. J. V. Gordon, R. E. Packard, *Phys. Rev. Lett.* **43**, 214 (1979).
3. K. W. Madison, F. Chevy, W. Wohlleben, J. Dalibard, *Phys. Rev. Lett.* **84**, 806 (2000).
4. ———, *J. Mod. Opt.* **47**, 2715 (2000).
5. P. O. Fedichev, A. E. Muryshev, preprint available at http://arXiv.org/abs/cond-mat/0004264.
6. Reviewed in A. L. Fetter, A. A. Svidzinsky, *J. Phys. Condens. Matter* **13**, R135 (2001).
7. M. R. Matthews *et al.*, *Phys. Rev. Lett.* **83**, 2498 (1999).
8. R. Onofrio *et al.*, *Phys. Rev. Lett.* **84**, 810 (2000).
9. M. R. Andrews, thesis, Massachusetts Institute of Technology (1998).
10. Reviewed in W. Ketterle, D. S. Durfee, D. M. Stamper-Kurn, in *Bose-Einstein Condensation in Atomic Gases, Proceedings of the International School of Physics Enrico Fermi, Course CXL*, M. Inguscio, S. Stringari, C. Wieman, Eds. (International Organisations Services B.V, Amsterdam, 1999), pp. 67–176.
11. E. Lundh, C. J. Pethick, H. Smith, *Phys. Rev. A* **58**, 4816 (1998).
12. F. Dalfovo, M. Modugno, *Phys. Rev. A* **61**, 023605 (2000).
13. Y. Castin, R. Dum, *Eur. Phys. J. D* **7**, 399 (1999).
14. R. Onofrio *et al.*, *Phys. Rev. Lett.* **85**, 2228 (2000).
15. M. R. Andrews *et al.*, *Science* **275**, 637 (1997).
16. A. A. Abrikosov, *J. Exp. Theor. Phys.* **5**, 1174 (1957) [*Zh. Eksp. Teor. Fiz.* **32**, 1442 (1957)].
17. V. K. Tkachenko, *J. Exp. Theor. Phys.* **22**, 1282 (1966) [*Zh. Eksp. Teor. Fiz.* **49**, 1875 (1965)].
18. P. Nozières, D. Pines, *The Theory of Quantum Liquids* (Addison-Wesley, Redwood City, CA, 1990).
19. K. W. Madison, F. Chevy, V. Bretin, J. Dalibard, preprint available at http://arXiv.org/abs/cond-mat/?0101051.
20. P. C. Haljan, B. P. Anderson, I. Coddington, E. A. Cornell, preprint available at http://arXiv.org/abs/cond-mat/0012320.
21. L. J. Campbell, R. M. Ziff, *Phys. Rev. B* **20**, 1886 (1979).
22. E. Lundh, C. J. Pethick, H. Smith, *Phys. Rev. A* **55**, 2126 (1997).
23. D. L. Feder, A. A. Svidzinsky, A. L. Fetter, C. W. Clark, *Phys. Rev. Lett.* **86**, 564 (2001).
24. J. J. García-Ripoll, V. M. Pérez-García, preprint available at http://arXiv.org/abs/cond-mat/0012071; ———, preprint available at http://arXiv.org/abs/con-mat/0101219.
25. T. Isoshima, K. Machida, *Phys. Rev. A* **60**, 3313 (1999).
26. A. A. Svidzinsky, A. L. Fetter, *Phys. Rev. Lett.* **84**, 5919 (2000).
27. F. Dalfovo, S. Giorgini, M. Guilleumas, L. P. Pitaevskii, S. Stringari, *Phys. Rev. A* **56**, 3840 (1997).
28. F. Dalfovo, S. Stringari, *Phys. Rev. A* **63**, 011601 (2001).
29. J. R. Anglin, personal communication.
30. C. Raman *et al.*, *Phys. Rev. Lett.* **83**, 2502 (1999).
31. R. J. Donnelly, *Quantized Vortices in Helium II* (Cambridge Univ. Press, Cambridge, 1991).
32. G. Blatter, M. V. Feigel'man, V. B. Geshkenbein, A. I. Larkin, V. M. Vinokur, *Rev. Mod. Phys.* **66**, 1125 (1994).
33. V. K. Tkachenko, *J. Exp. Theor. Phys.* **23**, 1049 (1966) [*Zh. Eksp. Teor. Fiz.* **50**, 1573 (1966)].
34. S. J. Tsakadze, *Fiz. Nizk. Temp.* **4**, 148 (1978) [*Sov. J. Low Temp. Phys.* **4**, 72 (1978)].

35. We thank J. R. Anglin, A. Görlitz, R. Onofrio, and L. Levitov for useful discussions and critical readings of the manuscript and T. Rosenband for assistance with the two-axis deflector. Supported by NSF, Office of Naval Research, Army Research Office, NASA, and the David and Lucile Packard Foundation.

26 February 2001; accepted 14 March 2001
Published online 22 March 2001;
10.1126/science.1060182
Include this information when citing this paper.

Self-Assembly of Subnanometer-Diameter Single-Wall MoS_2 Nanotubes

Maja Remskar,[1]* Ales Mrzel,[1] Zora Skraba,[1] Adolf Jesih,[1] Miran Ceh,[1] Jure Demšar,[1] Pierre Stadelmann,[2] Francis Lévy,[3] Dragan Mihailovic[1]

We report on the synthesis, structure, and self-assembly of single-wall subnanometer-diameter molybdenum disulfide tubes. The nanotubes are up to hundreds of micrometers long and display diverse self-assembly properties on different length scales, ranging from twisted bundles to regularly shaped "furry" forms. The bundles, which contain interstitial iodine, can be readily disassembled into individual molybdenum disulfide nanotubes. The synthesis was performed using a novel type of catalyzed transport reaction including C_{60} as a growth promoter.

The discovery of free-standing microscopic one-dimensional molecular structures, such as nanotubes of carbon, has attracted a great deal of attention in the last decade because of various interesting properties associated with their small dimensions, high anisotropy, and intriguing tube-like structures. These range from a variety of quantum effects (*1*, *2*) to potentially useful properties such as efficient field emission (*3*) and exceptional mechanical strength (*4*). Finding that curled-up dichalcogenide sheets can also form tube-like objects and fullerene-like nanoparticles (*5*–*8*) suggested that synthesis of nanotubes made of atoms other than carbon may be possible, and relatively small, 15-nm-diameter tubes made of tungsten and molybdenum disulfide have since been reported (*9*–*11*). The ultralow friction and wear properties of MoS_2 fullerene-like particles (*12*, *13*) make inorganic fullerenes important tribological materials. Other layered materials synthesized as nanotubes, tube-like forms, or onion-like structures have been reported, such as boron nitride nanotubes with diameters of a few nanometers (*14*, *15*), $W_{18}O_{49}$ hollow microfibers (*16*), and $NiCl_2$ multiwall nanotubes (*17*). Other layered compounds, such as NbS_2 (*18*) and GaSe (*19*), have been the subject of extensive theoretical calculations, which have predicted conditions for their stability in cylindrical form and some interesting electronic properties.

We report on the synthesis and basic structural properties of subnanometer-diameter monomolecular MoS_2 single-wall nanotubes (SWNTs) produced by a catalyzed transport reaction involving C_{60}, and show that the MoS_2 nanotubes grow in twisted chiral bundles of identically structured molecules stuck together with interstitial iodine. The tubes vary only in length, but not in diameter.

The single-wall MoS_2 nanotubes were grown by a catalyzed transport method using C_{60} as a growth promoter in the reaction. The C_{60} (5 weight %) was added to MoS_2 powder in the transport tube as catalyst, and the reaction was run typically for 22 days at 1010 K in an evacuated silica ampoule at a pressure of 10^{-3} Pa with a temperature gradient of 6 K/cm. Iodine was used as a transport agent. Approximately 15% (by weight) of the starting material was transported by the reaction to form SWNTs, with the rest remaining in the form of layered material. The transported material was subsequently thoroughly washed with toluene to remove the C_{60}.

The transported material grows in the form of bundles oriented perpendicular to the sub-

[1]Jozef Stefan Institute, Jamova 39, SI-1000 Ljubljana, Slovenia. [2]Centre de Microscopie Électronique-CIME, Ecole Polytechnique Fédérale de Lausanne, CH-1015 Lausanne, Switzerland. [3]Institute of Applied Physics, Ecole Polytechnique Fédérale de Lausanne, CH-1015 Lausanne, Switzerland.

*To whom correspondence should be addressed. E-mail: maja.remskar@ijs.si

strate surface (Fig. 1), consisting of individual MoS_2 nanotubes (*20*). These bundles start to grow from randomly distributed nucleation sites on the quartz surface. The bundles usually terminate in a sharp tip, forming sharp needles, with each bundle containing >500,000 ordered nanotubes. The secondary nucleation of the bundles on the rough top surface leads to the formation of microscopic geometrical shapes (Fig. 1, A and B). A well-pronounced self-assembly of the bundles indicates an attractive interaction among the nanotubes. Examination of the bundles reveals the presence of parallel-grown strands (Fig. 1C). These strands can be disassembled into thinner ones and even individual tubes by dispersion in ethanol using ultrasound (Fig. 1D).

Energy-dispersive x-ray spectroscopy (EDX) and x-ray fluorescence spectrometry have shown the chemical composition of the bundles to be (MoS_2)-I_x, with $x \approx 1/3$. Using energy electron loss spectrometer (EELS) analysis, we found no evidence that C_{60} is incorporated anywhere in the structure, suggesting that it only acts as a growth-promoting catalyst. The stability of the MoS_2 bundles at normal ambient conditions was evident from electron microscopy and diffraction, as well as from other techniques.

A high-resolution transmission electron microscopy (HRTEM) investigation of the bundles along their longitudinal direction revealed a hexagonal close-packing of identical nanotubes (Fig. 2), where the center-to-center distance between two tubes is 0.961(1) nm. HRTEM images taken approximately perpendicular to the nanotube axis reveal the ordered structure of individual nanotubes, as well as their regular stacking arrangement within the bundle (Fig. 1D and Fig. 3A).

Transmission electron diffraction (TED) shows a complex pattern with slightly deformed hexagonal symmetry (Fig. 3C). Perpendicular to the bundle axis, a period of 0.83(1) nm is dominant. This period is commensurate with regard to the period 0.27(1) nm belonging to the hexagonal pattern. Another strong peak situated close to the (030) spot is caused by a period of 0.30(1) nm. Two strong periods of 0.20(1) and 0.30(1) nm are present along the needle axis. X-ray diffraction confirms the TED data, revealing intense peaks corresponding to interlayer distances of 0.832(1), 0.351(1), 0.314(1), 0.308(1), 0.279(1), and 0.20(1) nm.

On the basis of the x-ray and electron diffraction data, we propose a model structure consisting of sulfur-molybdenum-sulfur cylinders (Fig. 2C and Fig. 3B). Following the usual nomenclature (*21*), the structure corresponds to a (3,3) armchair nanotube. In spite of the large

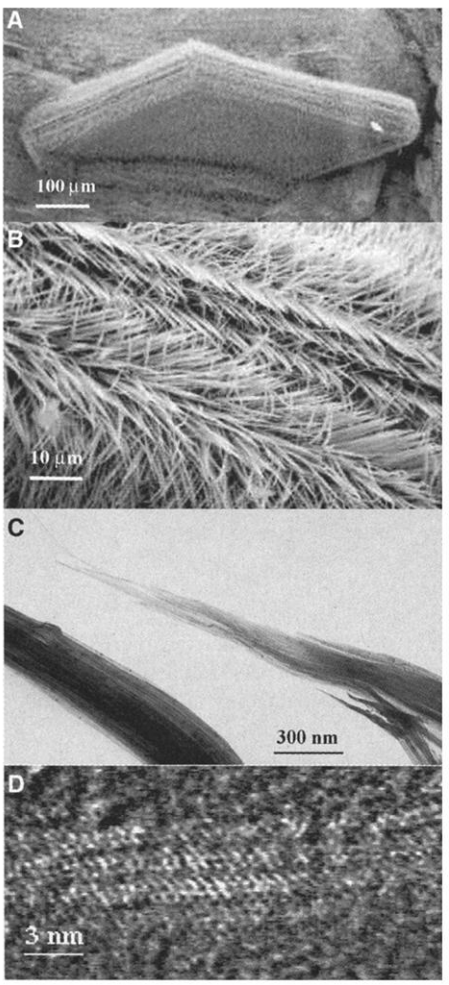

Fig. 1. Scanning electron and electron transmission images on different length scales. (**A**) Bundles appear to self-assemble into various different microscopic structures. (**B**) The bundles end in sharp points. (**C**) A split tip of a bundle terminating in strands ~4 nm wide. (**D**) Expanded electron transmission view of a strand composed of a only few individual nanotubes. The sample was prepared by dispersion in ethanol.

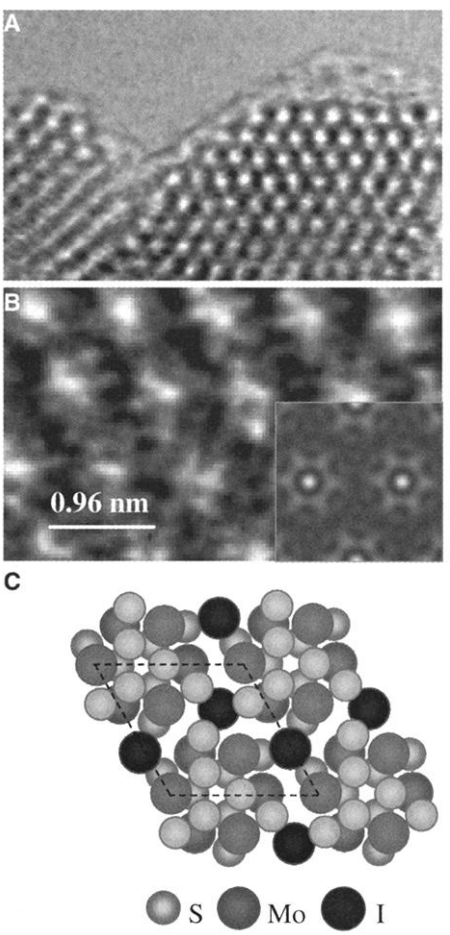

Fig. 2. TEM images of the cross section of a (MoS_2)-I_x bundle. (**A**) Hexagonal structure of the tubes within a bundle. (**B**) High-resolution view of the structure. The insert shows an image simulation for zone [001]. (**C**) A model structure perpendicular to the nanotube axis (gray, S; dark gray, Mo; black, I).

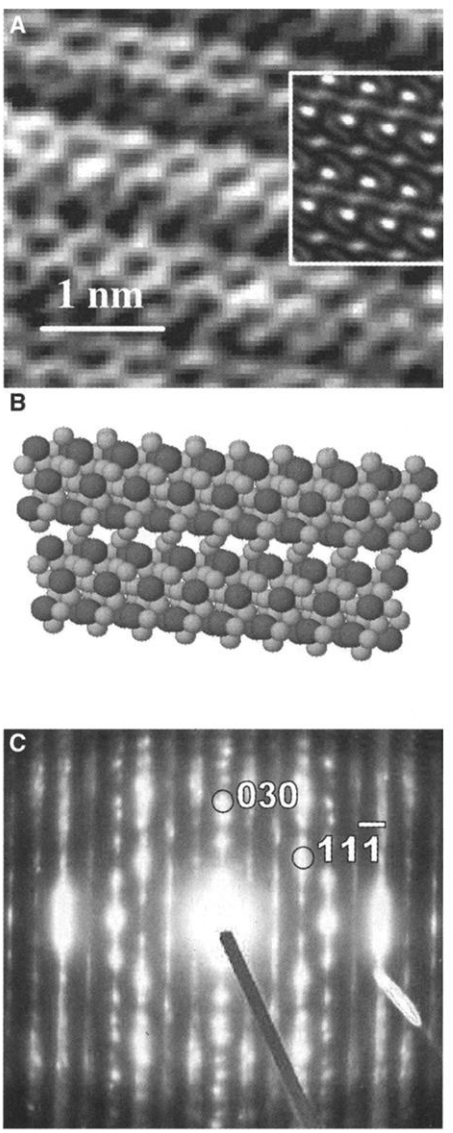

Fig. 3. TEM image and electron diffraction of the (MoS_2)-I_x bundle in zone [101]. (**A**) High-resolution image with image simulation revealing ordered stacking of nanotubes; bright spots correspond to the positions of molybdenum atoms. (**B**) Model structure of the tubes. (**C**) Corresponding electron diffraction pattern indexed in accordance with the model structure.

difference in circumferences, the distance between sulfur and molybdenum atoms in the nanotube is virtually equal to the corresponding distance in plate-like crystals of MoS_2 (*21*). The dihedral S-Mo-S angle is 63° and 66° for the inner and outer layers, respectively. For comparison, in plate-like crystals, the dihedral angle is 81.5° (*22*). The close position of molybdenum and sulfur atoms in neighboring layers perpendicular to the nanotube axis requires an extension of the unit cell along the tube axis by at least 25% to avoid overlap of the covalent radii. Considering such an extension, the distance between the layers is 0.20 nm, corresponding to the diffraction data.

The unit cell of the hexagonal close-packed nanotubes within a bundle is 0.40 nm along the bundle axis and 0.96 nm perpendicular to the bundle axis. The closest sulfur atoms on adjacent nanotubes are separated by 0.35(1) nm, which corresponds approximately to their Van der Waals diameters. Iodine atoms are inserted in interstitial trigonal voids between the nanotubes, creating one-dimensional rows along the bundle axis. The periodicity of feasible sites for iodine position along the bundle is 0.40 nm, which is slightly less than the Van der Waals distance for iodine (0.43 nm).

High-resolution simulations (Fig. 2B, inset, and Fig. 3A, inset) using the symmetry operations of Group $P6_3$ (C_6^6)–No. 173 are found in agreement with the observed high-resolution images. The unit cell contains 6 molybdenum atoms and 12 sulfur atoms. The electron diffraction pattern (Fig. 3C) is indexed using calculated interlayer distances of the model structure. A comparison of the interlayer distances measured by x-ray and electron diffraction with the calculated values is presented in Table 1.

The presence of C_{60} in the growth process was found to be essential, and the nanotubes do not grow in its absence, but the detailed growth mechanism is not clear at present. We remark on the fact that the (1,1,1) plane of C_{60} crystals shows a hexagonal pattern with the in-plane lattice parameter of 1.004 nm (*23*), which is a close, but not perfect, match to the nanotube crystal lattice shown in Fig. 2A. It is quite conceivable that C_{60} plays an active role in promoting growth at the tip of the growing nanotube.

Table 1. Comparison of x-ray and TED diffraction results. Assignment for a hexagonal lattice: a = 0.96(1) nm, c = 0.4 nm.

Measured *d* (nm) ± 0.01 nm	Calculated *d* (nm)	Assignment (hkl)
0.83	0.831	100
0.35	0.36	101
0.31	0.307	111
0.28	0.277	300
0.2	0.2	002

Recently, large-diameter armchair MoS_2 nanotubes were predicted on the basis of density-functional tight-binding calculations (*24*) to be semiconducting with either a direct or an indirect bandgap, depending on their diameter and structure. Extrapolating these predictions to the (3,3) tubes discussed here, we can expect the indirect gap to close, giving rise to a metal with a small, but finite, density of states at E_F. However, the effect of confinement of electrons on the very narrow tubes is expected to give rise to energy level quantization for electrons hopping perpendicular to the tube axis which, because of the small diameters, may be expected to persist to unusually high temperatures.

Because of their efficient growth properties, the tubes may give rise to a new chalcogenide-nanotube technology based on their low-dimensional properties. The self-assembly into various regular geometrical shapes on different length scales appears to be a property unique to the MoS_2 SWNTs. The possibility of handling single tubes, such as was already demonstrated here, should facilitate investigation of single-tube properties, including quantum effects, in more detail.

References and Notes

1. M. Bockrath *et al.*, *Nature* **397**, 598 (1999).
2. A. Bachtold *et al.*, *Nature* **389**, 582 (1999).
3. W. A. de Heer, A. Châtelain, D. Ugarte, *Science* **270**, 1179 (1995).
4. M. M. J. Treacy, T. W. Ebbesen, J. M. Gibson, *Nature* **381**, 678 (1996).
5. R. Tenne *et al.*, *Nature* **360**, 444 (1992).
6. L. Margulis *et al.*, *Nature* **365**, 113 (1993).
7. R. Tenne *et al.*, *Chem. Mater.* **10**, 3225 (1999).
8. A. Zak, Y. Feldman, V. Alperovich, R. Rosentsveig, R. Tenne, *J. Am. Chem. Soc.* **122**, 11108 (2000).
9. M. Remskar, Z. Skraba, F. Cleton, R. Sanjines, F. Levy, *Appl. Phys. Lett.* **69**, 351 (1996).
10. M. Remskar *et al.*, *Adv. Mater.* **10**, 246 (1998).
11. M. Remskar, Z. Skraba, R. Sanjines, F. Levy, *Appl. Phys. Lett.* **74**, 633 (1999).
12. Y. Golan *et al.*, *Adv. Mater.* **11**, 934 (1999).
13. M. Chhowalla, G. A. J. Amaratunga, *Nature* **407**, 164 (2000).
14. N. G. Chopra *et al.*, *Science* **269**, 966 (1995).
15. M. Terrones *et al.*, *Chem. Phys. Lett.* **259**, 568 (1996).
16. W. B. Hu *et al.*, *Appl. Phys. A* **70**, 231 (2000).
17. Y. Rosenfeld Hacohen, E. Grunbaum, R. Tenne, J. Sloan, J. L. Hutchison, *Nature* **395**, 336 (1998).
18. G. Seifert, H. Terrones, M. Terrones, T. Frauenheim, *Solid State Commun.* **115**, 635 (2000).
19. M. Côté, M. L. Cohen, D. J. Chadi, *Phys. Rev. B* **58**, R4277 (1998).
20. The structure of the transported material was studied using 300-keV Philips CM300, Jeol JEM-2010F, and Philips XL 30FEG electron microscopes and Hitachi HF-2000 equipped with EELS. X-ray structural analysis has been used for confirmation of electron diffraction data and x-ray fluorescence spectrometry for composition analysis.
21. M. S. Dresselhaus, G. Dresselhaus, P. C. Ecklund, *Science of Fullerenes and Carbon Nanotubes* (Academic Press, New York, 1996).
22. J. A. Wilson, A. D. Yoffe, *Adv. Phys.* **18**, 193 (1969).
23. W. Krätschmer, L. D. Lamb, K. Fostiropoulos, D. R. Huffman, *Nature* **347**, 354 (1990).
24. G. Siefert, H. Terrones, M. Terrones, G. Jungnickel, T. Frauenheim, *Phys. Rev. Lett.* **85**, 146 (2000).

25. We thank M. Cantoni and G. Drazic for help in electron microscopy and P. Kump for x-ray fluorescence measurements. We are also sincerely grateful G. Seifert and H. Cohen for useful discussions.

12 January 2001; accepted 9 March 2001

Probing the Structure of Metal Cluster–Adsorbate Systems with High-Resolution Infrared Spectroscopy

K. Nauta, D. T. Moore, P. L. Stiles, R. E. Miller*

High-resolution infrared laser spectroscopy was used to obtain rotationally resolved infrared spectra of adsorbate-metal complexes. The method involves forming the bare metal clusters in helium nanodroplets and then adding a molecular adsorbate (HCN) and recording the infrared spectrum associated with the C-H stretching vibration. Rotationally resolved spectra were obtained for HCN-Mg_n (n = 1 to 4). The results suggest a qualitative change in the adsorbate–metal cluster bonding with cluster size.

The vibrational dynamics of molecules adsorbed on metal surfaces is of fundamental interest (*1*) and great practical importance to several fields, for example, catalysis (*2*, *3*). Infrared (IR) spectroscopy has been widely used to study such processes (*1*), with the goal of understanding the associated molecule-surface interactions. Although studies of this type have provided important insights into the nature of the associated interactions, progress has been hampered because the theoretical methods used to interpret the experimental data have trouble dealing with the large number of surface atoms (*4*). In most cases, this problem has been addressed by

Department of Chemistry, University of North Carolina, Chapel Hill, NC 27599, USA.

*To whom correspondence should be addressed. E-mail: remiller@unc.edu